

# International Journal of Advanced Manufacturing Technology

## Microstructural aspects in Al-Cu dissimilar joining by FSW

--Manuscript Draft--

<b>Manuscript Number:</b>	
<b>Full Title:</b>	Microstructural aspects in Al-Cu dissimilar joining by FSW
<b>Article Type:</b>	Original Research
<b>Keywords:</b>	friction stir welding; dissimilar joint; AA2024-T3; Cu10100; microstructure; EDS
<b>Corresponding Author:</b>	Pierpaolo Carlone, Ph.D. University of Salerno Fisciano, ITALY
<b>Corresponding Author Secondary Information:</b>	
<b>Corresponding Author's Institution:</b>	University of Salerno
<b>Corresponding Author's Secondary Institution:</b>	
<b>First Author:</b>	Pierpaolo Carlone, Ph.D.
<b>First Author Secondary Information:</b>	
<b>Order of Authors:</b>	Pierpaolo Carlone, Ph.D. Antonello Astarita, Ph.D. Gaetano Salvatore Palazzo Valentino Paradiso, Ph.D. Antonino Squillace, Ph.D.
<b>Order of Authors Secondary Information:</b>	
<b>Abstract:</b>	Sound AA2024-T3 - Cu10100 dissimilar joints were obtained by friction stir welding offsetting the tool pin towards the aluminum sheet and employing selected processing parameters. Joint microstructure was analyzed by means of conventional optic microscopy as well as scanning electron microscopy. The weld bead exhibited welding zones and some features typically encountered in similar FSW. The nugget zone consisted of a mixture of recrystallized aluminum matrix and deformed and twinned copper particles. Onion rings and particles-rich zones, made of Cu particles dispersed in the Al matrix, were also observed. EDS analysis revealed that several Al-Cu intermetallic compounds, such as Al <sub>2</sub> Cu, AlCu, and Al <sub>3</sub> Cu <sub>4</sub> , chemically different w.r.t. compounds precipitated during the T3 aging treatment (Al <sub>3</sub> Cu), were formed during the process. Microstructure variation significantly affects the microhardness distribution in the cross section of the joint.
<b>Suggested Reviewers:</b>	Dulce M.E. Rodrigues , Ph.D. Professor, University of Coimbra dulce.rodrigues@dem.uc.pt Expert in dissimilar joining by FSW and other welding processes
	Gianluca Buffa, Ph.D. Assistant Professor, University of Palermo gianluca.buffa@unipa.it Expert in mechanical and microstructural analysis of friction stir welded joints
	Adrian Murphy, Ph.D. Professor, Queen's University Belfast a.murphy@qub.ac.uk Expert in manufacturing and joining (including FSW) processes for aerospace applications
	Cem C. Tutum, Ph.D.

	Professor, Michigan State University tutum@msu.edu Expert in FSW process of aluminum alloys
--	---

Dear Editor,

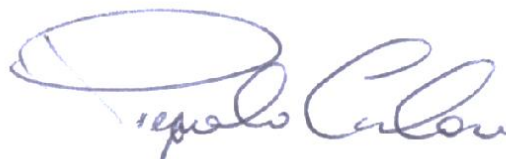
Please find enclosed our manuscript, "Microstructural aspects in Al–Cu dissimilar joining by FSW" by Pierpaolo Carlone, Antonello Astarita, Gaetano S. Palazzo, Valentino Paradiso, Antonino Squillace, which we would like to submit for publication as an original research paper in International Journal of Advanced Manufacturing Technology.

Although the Friction Stir Welding process has been/is the subject of very intensive researches and several reports, mostly dealing with similar aluminum joining, are already available in the literature, very few investigations are focused on the dissimilar joining of aluminum alloy to copper by FSW. To our best knowledge, this is the first work detailing the application of the process to join AA2024-T3, which is widely used for aeronautical applications, to Cu10100. In particular, attention was focused on some microstructural aspects inherent the welding zone. Taking into account the novelty of the work and the interest in the considered materials, we are confident that the paper would appeal to the industrial as well as academic readership of International Journal of Advanced Manufacturing Technology.

We confirm that this manuscript has not been published, accepted, or submitted for publication elsewhere. No earlier version of this paper has been presented elsewhere. No other paper has been published using the same data set.

Best Regards,

Pierpaolo Carlone, PhD  
Department of Industrial Engineering  
University of Salerno



# Microstructural aspects in Al–Cu dissimilar joining by FSW

Pierpaolo Carlone<sup>1</sup>, Antonello Astarita<sup>2</sup>, Gaetano S. Palazzo<sup>1</sup>, Valentino Paradiso<sup>2</sup>, Antonino Squillace<sup>2</sup>

<sup>1</sup>Department of Industrial Engineering, University of Salerno, Via Giovanni Paolo II 132, 84084 Fisciano (SA), Italy

<sup>2</sup>Department of Chemical, Materials and Industrial Production Engineering, University of Naples “Federico II”, P.le Tecchio 80, 80100 Naples, Italy

## Abstract.

Sound AA2024-T3 – Cu10100 dissimilar joints were obtained by friction stir welding offsetting the tool pin towards the aluminum sheet and employing selected processing parameters. Joint microstructure was analyzed by means of conventional optic microscopy as well as scanning electron microscopy. The weld bead exhibited welding zones and some features typically encountered in similar FSW. The nugget zone consisted of a mixture of recrystallized aluminum matrix and deformed and twinned copper particles. Onion rings and particles-rich zones, made of Cu particles dispersed in the Al matrix, were also observed. EDS analysis revealed that several Al-Cu intermetallic compounds, such as Al<sub>2</sub>Cu, AlCu, and Al<sub>3</sub>Cu<sub>4</sub>, chemically different w.r.t. compounds precipitated during the T3 aging treatment (Al<sub>3</sub>Cu), were formed during the process. Microstructure variation significantly affects the microhardness distribution in the cross section of the joint.

**Keywords:** friction stir welding, dissimilar joint, AA2024-T3, Cu10100, microstructure, EDS

## 1. Introduction

1  
2 Dissimilar joining of aluminum to copper is gaining a great deal of attention in several applicative  
3  
4 sectors. The intriguing advantages achievable in terms of weight saving and cost reduction make this  
5  
6 combination of materials very appealing for the chemical, aerospace, transportation, and electronics  
7  
8 industries [1-3]. Due to the difficulties in making an electrically stable bolted hybrid joint, much  
9  
10 effort has been focused on welding aluminum to copper in the last decades [4].  
11  
12

13  
14 Previous literature [5] pointed out that the joining of such dissimilar materials by fusion welding  
15  
16 processes is quite challenging due to their different chemical, mechanical, thermal properties. The  
17  
18 melting points of aluminum and copper differ of about nearly 400 °C. This may result in remarkable  
19  
20 non-homogeneities in the microstructure of the adjoined materials, negatively affecting the overall  
21  
22 joint performance. Indeed, aluminum is easily oxidized at elevated temperatures, and welding cracks  
23  
24 are commonly detected in brazed or fusion welded Cu joints [6]. What is more, during fusion  
25  
26 welding or pressure welding (brazing, diffusion bonding, etc) of Cu/Al some issues concerning the  
27  
28 formation of hard and brittle intermetallic compounds (IMCs) in large scale at weld interface were  
29  
30 pointed out by the experimental analysis reported by Liu et al. [7]. These IMCs could lead to a  
31  
32 decreasing of the mechanical properties of the entire joint [8].  
33  
34  
35  
36  
37

38  
39 In recent years, solid-state joining techniques, such as friction welding, roll welding, and explosive  
40  
41 welding have received much interest for such applications [9-11]. Among others, a great deal of  
42  
43 attention is directed towards the friction stir welding process (FSW). Some researchers studied the  
44  
45 FSW of Al-Cu dissimilar joints, focusing on pure aluminum and cast aluminum alloys [12]. The  
46  
47 literature converges on two general aspects: i. sound dissimilar FSW Al-Cu joints are difficult to  
48  
49 achieve and ii. a key role is played by the brittle IMCs formed in the nugget zone (NZ). According  
50  
51 to the experimental analysis performed by Murr et al. [3], Al-Cu joints generally fail at the NZ or  
52  
53 along the interface between the two materials during the mechanical tests [13]. Ouyang et al. [1]  
54  
55 attributed the poor weldability to various brittle IMCs formed in the NZ. Lee and Jung [14]  
56  
57 suggested that the formation of  $Al_2O_3$  and CuO layers resulted in lower tensile strength attributable  
58  
59  
60  
61  
62  
63  
64  
65

1 to the presence of brittle IMCs. In a previous study [15], sound FSW Al–Cu joints were obtained by  
2 offsetting the tool to the aluminum side under a lower heat input condition. The formation of a thin,  
3  
4 continuous and uniform IMCs layer created an excellent metallurgical bonding at Al–Cu interface,  
5  
6 and no oxide layer was found. It is well documented that several parameters, such as tool offsetting,  
7  
8 rotation rate and traverse speed, influenced the weld properties of the dissimilar FSW joints [16–19].  
9  
10 Despite the number of articles available on this topic there are very few papers dealing with the  
11  
12 dissimilar welding between copper and the high strength aluminum alloys, such as 2XXX (Al-Cu)  
13  
14 series. In particular the AA2024 Al-Cu alloy is widely used for structural application in aeronautics  
15  
16 [20,21]. Due to the presence of copper precipitates at the grain boundaries, this alloy is expected to  
17  
18 easily form IMCs with the copper during the FSW process. Moreover its hardening mechanism is  
19  
20 based on the formation of Al-Cu precipitates (in particular  $Al_3Cu$ ) in the Al lattice, preventing the  
21  
22 dislocations migration and enhancing the mechanical properties [22]. This paper studies the  
23  
24 dissimilar joining by FSW between pure copper (Cu10100) and the high strength aluminum alloy  
25  
26 AA2024-T3. Due to the aforementioned reasons, the AA2024 – Cu10100 joining by FSW is  
27  
28 expected to produce a weld bead with a very complex metallurgy. The aims of this paper are to  
29  
30 prove the capability of the FSW process to provide sound joints and to study the microstructure and  
31  
32 the metallurgy of the joint.  
33  
34  
35  
36  
37  
38  
39  
40  
41  
42

## 43 **2. Experimental**

44  
45 AA2024-T3 rolled sheet and pure Cu10100 rolled and cold drawn sheet were used as base material.  
46  
47 The chemical composition and the main mechanical properties of the two alloys are fully available  
48  
49 elsewhere [23,24] and are not reported here in the interest of brevity. The in plane dimensions of the  
50  
51 adjoining sheets were 120 mm x 30 mm, while thickness was 2 mm. AA2024 sheet was fixed in the  
52  
53 advancing side of the joint and the tool was displaced towards the aluminium side (i.e. the harder  
54  
55 material) of a predefined offset. A scheme of the welding configuration, including also a detail of  
56  
57 the tool, is provided in figure 1.  
58  
59  
60  
61  
62  
63  
64  
65

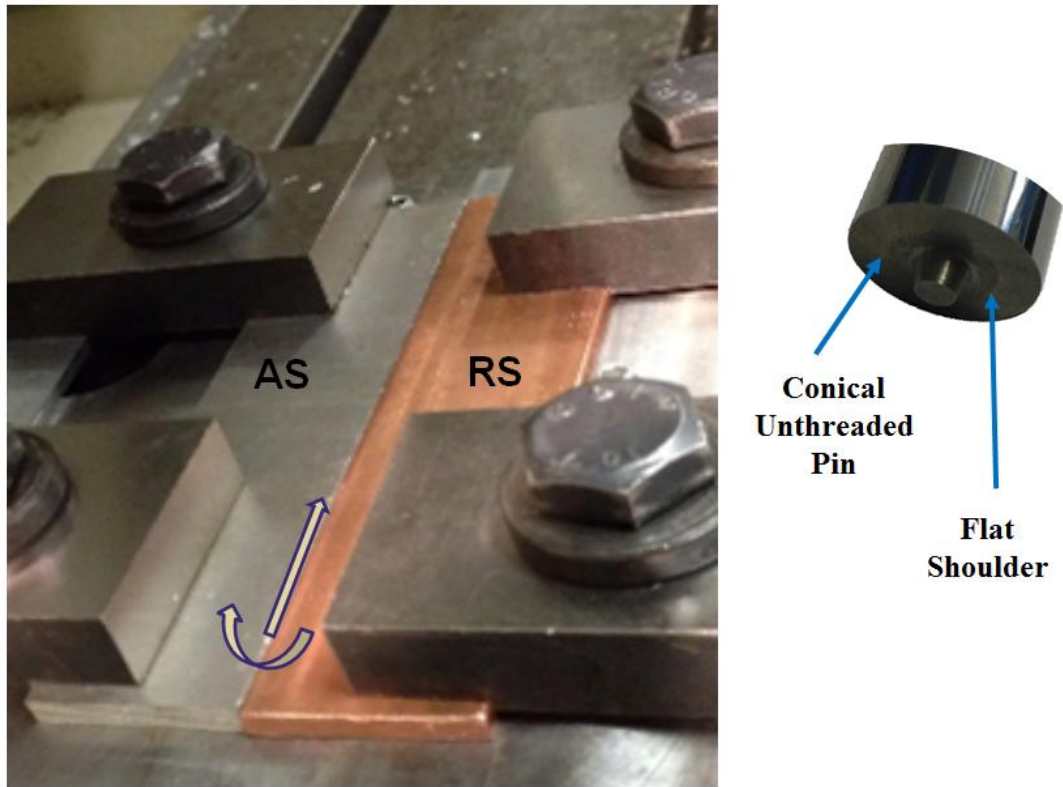


Fig. 1 FSW process setup and tool.

Non-consumable tools, made of Cr-Mo steel, were used to fabricate the joints. Tool geometry is characterised by a shoulder diameter of 20 mm and by an unthreaded conical pin with 5.2 mm major diameter, 15° cone angle and 1.8 mm length. The forging action of the tool shoulder was enhanced imposing a tilt angle of 2°. The plates were welded using a machining centre MCX 600 ECO. Process parameters were chosen on the basis of the available literature and comparing the process windows obtained welding singularly AA2024-T3 and Cu10100 [25,26]. Furthermore, a preliminary test campaign was performed by trial and error before the achievement of material continuity. The employed parameters are given in table 1.

Table 1 – FSW process parameters.

Rotational speed (rpm)	Welding speed (mm/min)	Tilt angle (°)	Tool offset (mm)
1000	80	2	1.3

1 The welding process was carried out following plunging, dwelling, and welding phases. The feed  
2 rate of the tool along the vertical axis during the plunging phase was set as 5 mm/min, while the  
3 duration of dwell was set as 10 seconds. Three different joints were carried out in order to ensure the  
4 repeatability of the process. The microstructure of the joint was studied through metallographic  
5 observations by means of both light optical microscope and scanning electron microscope (SEM).  
6 Moreover, chemical composition measurements were carried out through an EDS probe to study the  
7 IMCs generated by the welding process. In more details, each specimen was cold mounted in a  
8 proper thermoset resin and polished with grinding discs (P320, P600, P1200, P2000) and  
9 polycrystalline diamond suspension (3 $\mu$ m) on tissue disc until the surface exhibited a mirror like  
10 finish. Afterward, the samples were etched by a modified Keller's reagent (150 ml H<sub>2</sub>O, 2 ml HNO<sub>3</sub>,  
11 6 ml HCl, 6 ml HF) to unveil the significant features of the aluminium metallurgical  
12 microstructures. The same procedure has been repeated to investigate the copper microstructures  
13 using a solution of 30 ml HCl, 40 ml HNO<sub>3</sub>, 2.5 ml HF, 12 g C<sub>2</sub>O<sub>2</sub> and 42.5 ml H<sub>2</sub>O. Optical  
14 observations were performed using a metallurgical microscope equipped with a Nikon digital  
15 camera to evaluate the weld bead morphology. SEM observations and EDS measurements were  
16 carried out through an Hitachi TM3000 table top SEM equipped with a National Instruments EDS  
17 probe. Vickers micro hardness was measured in the cross section of the joint by means of a LEICA  
18 VMHT AUTO machine in order to assess the influence of the microstructure on the mechanical  
19 properties of the joint itself. Three linear patterns, orthogonal to the weld line, were programmed,  
20 respectively at the mid-thickness of the joint cross section and at a distance equal to 0.5 mm toward  
21 the top and bottom surfaces. The following parameters were adopted: distance between two  
22 consecutive indentations 1 mm, indentation load 50 gf (0.49N), loading time 15 sec, and indentation  
23 speed 60  $\mu$ m/sec.

### 3. Results and discussion

24 The surface morphology of the joint is shown in Figure 2. Sound weld surfaces were achieved

1 adopting the aforementioned welding configuration and parameters. In this regard, it is worth to  
2 point out that in preliminary FSW tests, tunnel defects, as well as surface defects (i.e. groove, flash,  
3 instability of the welding path), were observed reverting the position of the two sheets even reducing  
4 the welding speed. Figure 2 shows also the cross-sectional macrograph obtained after etching.  
5  
6 Satisfactory material continuity was exhibited in the weld bead. The stirring experienced by the  
7 material during the process is well appreciable in the same figure. As can be seen, copper  
8 experienced a higher deformation than aluminum. Indeed, the softened copper, stirred by the pin  
9 action, penetrates into the aluminum sheet. The plastic flow of the copper is clearly evident looking  
10 at the remixed copper hook in Figure 2, creating a sort of mechanical bond between the two  
11 materials. This allows affirming that fixing the harder plate (AA 2024 in this study) in the advancing  
12 side of the joint during dissimilar FSW is one of the key factors providing sound weld quality.  
13  
14

15 The following explanation is provided. During FSW process, adjoining material is transferred from  
16 the retreating side to the advancing side behind the pin, where the weld bead is formed [27,28].  
17  
18 When the softer material is fixed at the retreating side, it is easily forced towards the advancing side.  
19  
20 Being the hardness of the AA2024 higher than that of the Cu10100, an enhanced material flow in  
21 the soft copper base is reasonably expected [29]. What is more, previous studies indicated that the  
22 weld quality in dissimilar FSW joints is strongly influenced by the offsetting of the pin [30]. Similar  
23 considerations apply to other materials pairs. For instance, Watanabe et al. [17] reported that long  
24 crack line was observed on the crown of FSW Al-Fe joints when the Fe (i.e. the harder material) was  
25 fixed in the retreating side, and sound weld surface could be obtained in reversed fixing conditions.  
26  
27  
28  
29  
30  
31  
32  
33  
34  
35  
36  
37  
38  
39  
40  
41  
42  
43  
44  
45  
46  
47  
48  
49  
50  
51  
52  
53  
54  
55  
56  
57  
58  
59  
60  
61  
62  
63  
64  
65

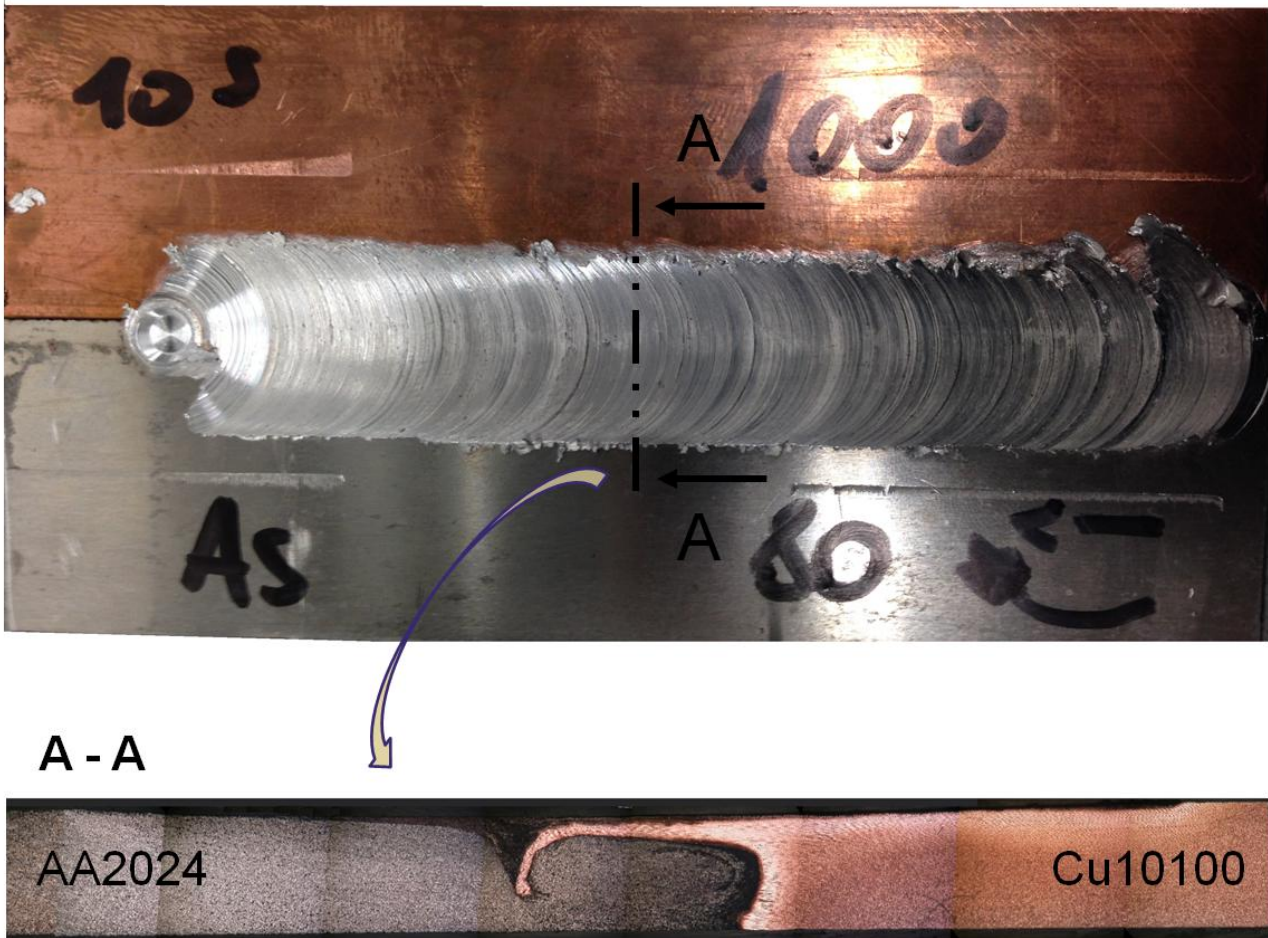


Fig. 2 Surface morphology of the joint (top) and cross section macrograph of the joint (bottom).

Figure 3 shows the SEM macroscopic appearance and microstructures of the Al–Cu joint. The NZ consists of a mixture of aluminum matrix and Cu particles. Many fine particles with various sizes and irregular shapes were dispersed in the Al matrix; large particles were also observed. The distribution of Cu particles appeared inhomogeneous in the NZ and a particles-rich zone (PRZ) was also detected near the bottom. Thus, the NZ can be considered an aluminum matrix composite with both Cu particles and Al-Cu intermetallic dispersed within. The presence of this structure is attributable to the stirring action of the tool pin, which scraped Cu pieces from the bulk copper, breaking up and dispersing them during FSW process. Typical onion rings, made of Cu particles dispersed in the Al matrix, were also detected. Intriguingly, a remixing zone (RZ) resembling the typical thermo-mechanically affected zone (TMAZ) zone observed in similar FSW butt joints was

individuated (Figure 3) and related to diffusion phenomena induced by thermo-mechanical loads experienced by the adjoining materials.

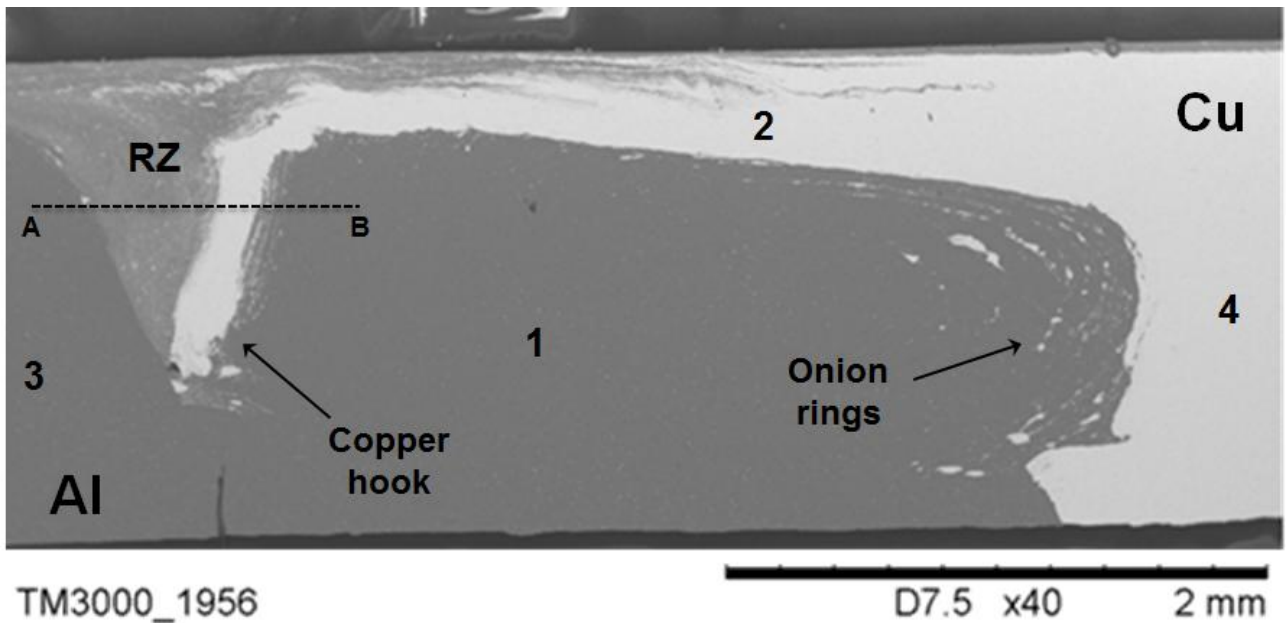
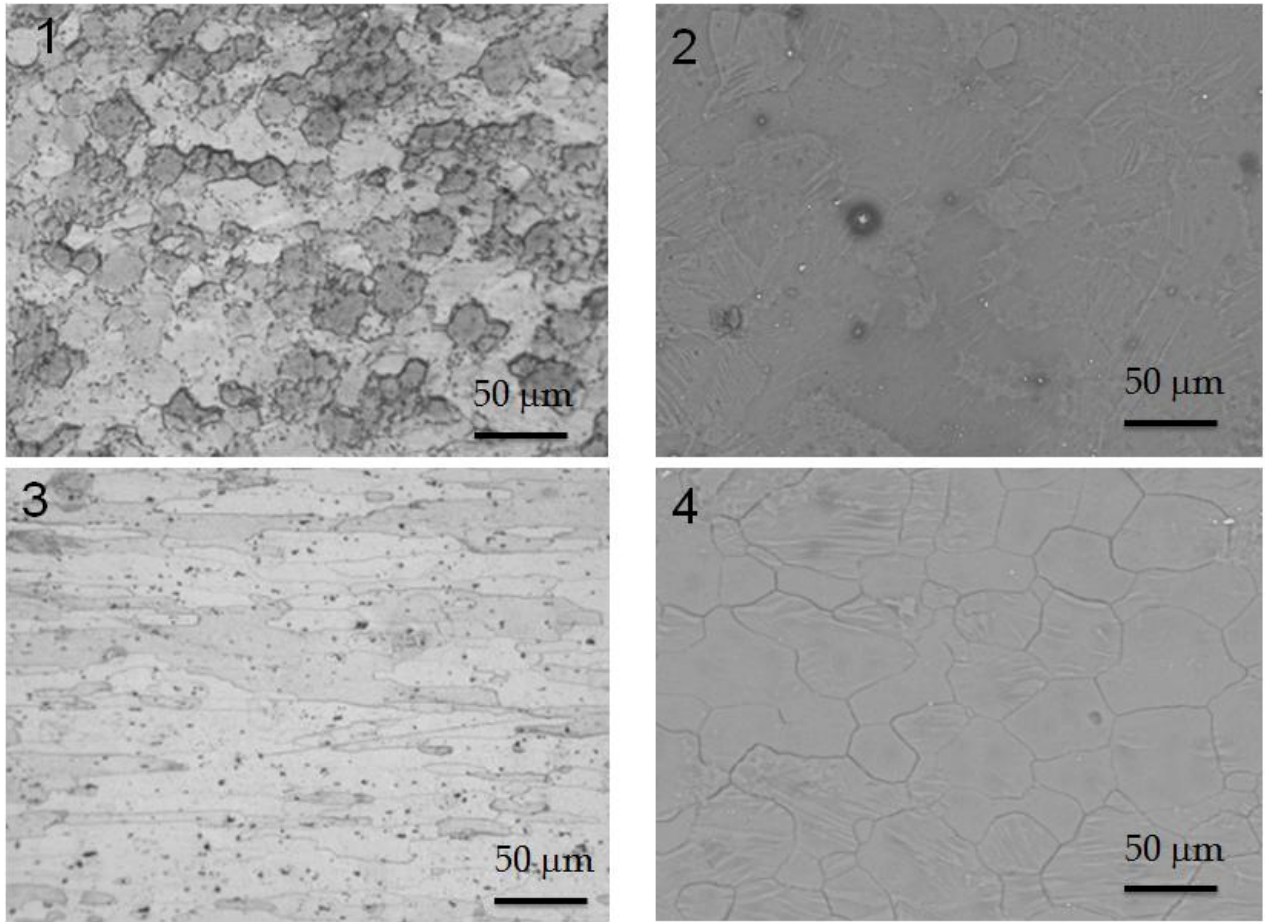


Fig. 3 SEM macrograph of the cross section of the weld bead.

In Figure 4, microstructures observed in the stirred materials (points 1 and 2, as indicated in Figure 3) as well as in the undeformed base materials (point 3 and 4, as indicated in Figure 3) are reported. Figure 4.1 depicts the microstructure in the NZ. In this zone, due to the thermo-mechanical action of the tool, the microstructure was fully recrystallized resulting in the fine equiaxial grains with average grain diameter equal to 30  $\mu\text{m}$ . In figure 4.2 the microstructure observed in the point 2 of figure 3 is reported. In these zone copper experienced a severe plastic flow but the heat input was too low to achieve a fully recrystallization. As a consequence, the mean grain dimension was similar to the one of the parent material, with an average diameter of approximately 50  $\mu\text{m}$ . However, the stirring effect induced very deformed and twinned grains, characterized by low defined borders. Concerning the Al in the zone external to the weld bead (Figure 4.3), it is appreciable the typical microstructure of the rolled AA2024 after the T3 aging treatment. Pancake elongated grains were exhibited, with the presence of the  $\text{Al}_3\text{Cu}$  precipitates. Moreover second phase black particles were also visible, exhibiting typical composition encountered in 2XXX aluminum alloys (that is rich in

1  
2 Fe, Cu, Mg, and Mn). The microstructure of the Cu10100, externally to the stirred zone, showed the  
3 typical features induced by the cold drawing process, with the presence of some deformed grains  
4 (Figure 4.4).  
5  
6



47  
48  
49  
50  
51  
52  
53  
54  
55  
56  
57  
58  
59  
60  
61  
62  
63  
64  
65

Fig. 4 Microstructure of joint: NZ (1); deformed Cu (2); undeformed AA2024-T3 (3); undeformed Cu10100 (4).

As far the IMCs precipitation is regarded, according to the Al–Cu binary equilibrium phase diagram [31], several Al–Cu particles, including  $Al_2Cu$ ,  $AlCu$ ,  $Al_3Cu_4$ , may be developed during the Al/Cu process induced reaction. Some studies indicated that Al-rich phase  $Al_2Cu$  and Cu-rich phase  $Al_4Cu_9$  were the first two IMCs formed adjacent to Al side and Cu side, respectively [32-34]. However, it should be borne in mind that the AA2024 base material used in this work was rich of  $Al_3Cu$  precipitates due to the T3 heat treatment, so it is important to distinguish these particles from IMCs

1 developed during the welding process. The presence of the above cited IMCs in the NZ was clearly  
 2 highlighted by EDS measurements. As aforementioned, these particles affect the mechanical  
 3 behavior of the joint [35,36]. The EDS analysis also confirmed that these particles differ from the  
 4 ones precipitated during the heat treatment. In Figure 5 a magnification of the PRZ zone is reported,  
 5 showing several Cu particles dispersed in the aluminum matrix. The chemical composition of these  
 6 particles ( $\text{Al}_2\text{Cu}$ ,  $\text{AlCu}$ ,  $\text{Al}_3\text{Cu}_4$ ), given in table 2, evidently differs from the one exhibited by  
 7  $\text{Al}_3\text{Cu}$  particles precipitated during the ageing phase of the heat treatment.

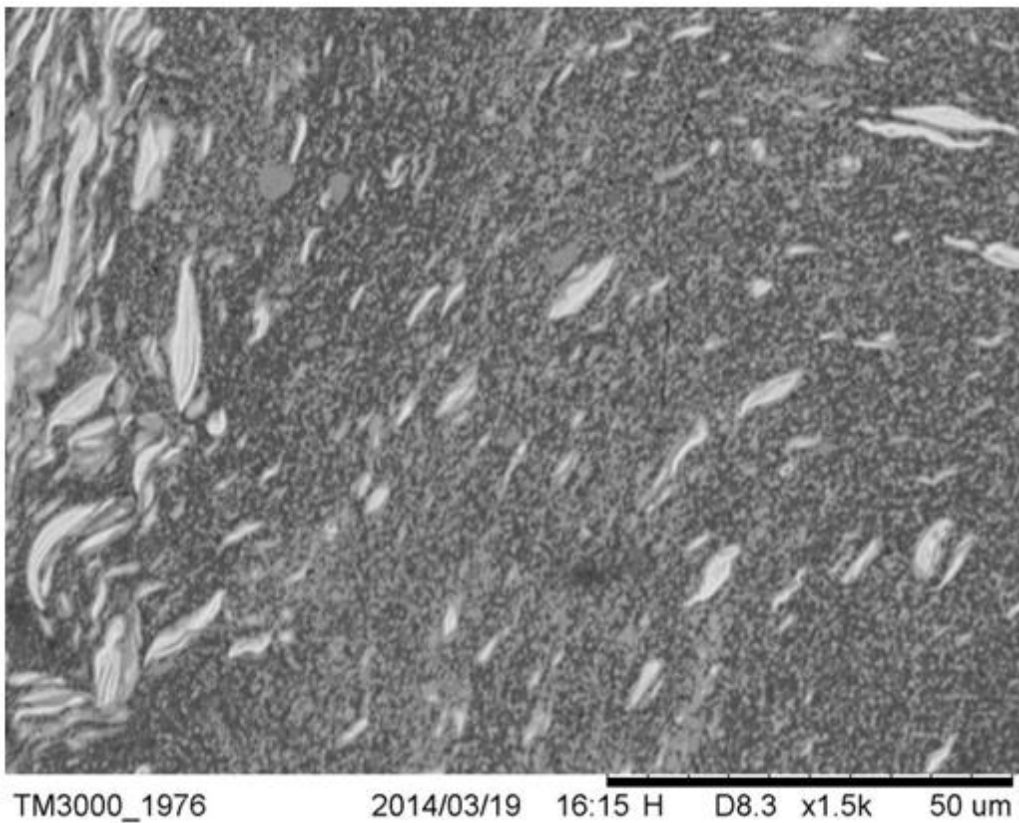


Fig. 5 Magnification of the PRZ zone (Cu particles are brighter than the Al matrix).

Table 2 – Chemical composition of IMCs precipitated during FSW process and detected in the NZ

IMC	Al (%)	Cu (%)
$\text{AlCu}$	52	48
$\text{Al}_2\text{Cu}$	65	35
$\text{Al}_3\text{Cu}_4$	42	58
$\text{Al}_3\text{Cu}$	76	24

1  
2 Figure 6 shows aluminum and copper intensity, as measured through EDS analysis, along the scan  
3  
4 line AB, as depicted in Figure 4. Please note that intensity values were normalized for both elements  
5  
6 with respect to the maximum peak intensity in order to improve the readability of the plot. The  
7  
8 variability of the presence of aluminum and copper can be well appreciated, confirming that in this  
9  
10 zone the stirring action induced an intimately remixing between the two materials and a quite non-  
11  
12 homogeneous microstructure. More specifically, at the beginning of the scan line, in correspondence  
13  
14 of the undeformed aluminum, the chemical composition reflects the typical AA2024 one. Al  
15  
16 percentage gradually drops with a contemporary increase of the Cu percentage approaching the RZ.  
17  
18 Some abnormal peaks in the copper profile evidence the presence of large copper particles or  
19  
20 lamellae dispersed in the aluminum. Then, a segment characterized by the predominant presence of  
21  
22 copper is encountered, corresponding to the copper hook. As shown, the aluminum content  
23  
24 completely vanishes, confirming that this hook was roughly created by the copper stirred and  
25  
26 deposited on the advancing side of the weld. Beyond this formation, Al content increases and Cu  
27  
28 content decreases following a marked oscillating behavior, resembling sort of a layered Al-Cu  
29  
30 deposition. Finally, in the NZ, aluminum content results minor with respect to the parent material,  
31  
32 due to the copper particles dispersed therein.  
33  
34  
35  
36  
37  
38  
39  
40  
41  
42  
43  
44  
45  
46  
47  
48  
49  
50  
51  
52  
53  
54  
55  
56  
57  
58  
59  
60  
61  
62  
63  
64  
65

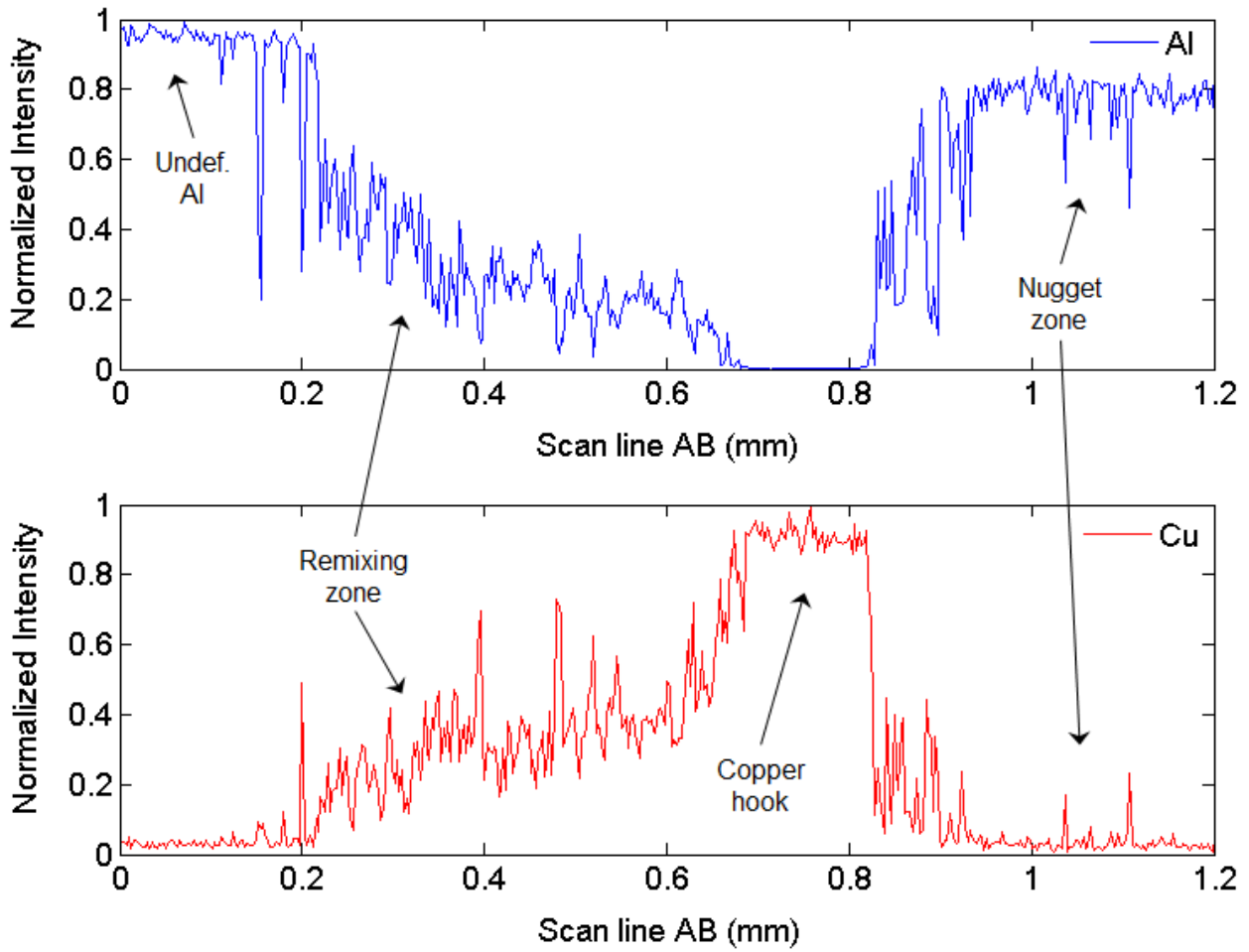


Fig. 6 Al and Cu intensity, as measured along the line AB depicted in Figure 4

In figure 7 a micrograph of transition zone in the retreating (copper) side is reported. Some cracks due to the stirring and scratching action of the pin are appreciable. As generally accepted, the presence of these cracks reduces the mechanical properties of the joint, however it is generally considered a peculiar feature of this kind of dissimilar joints [16].

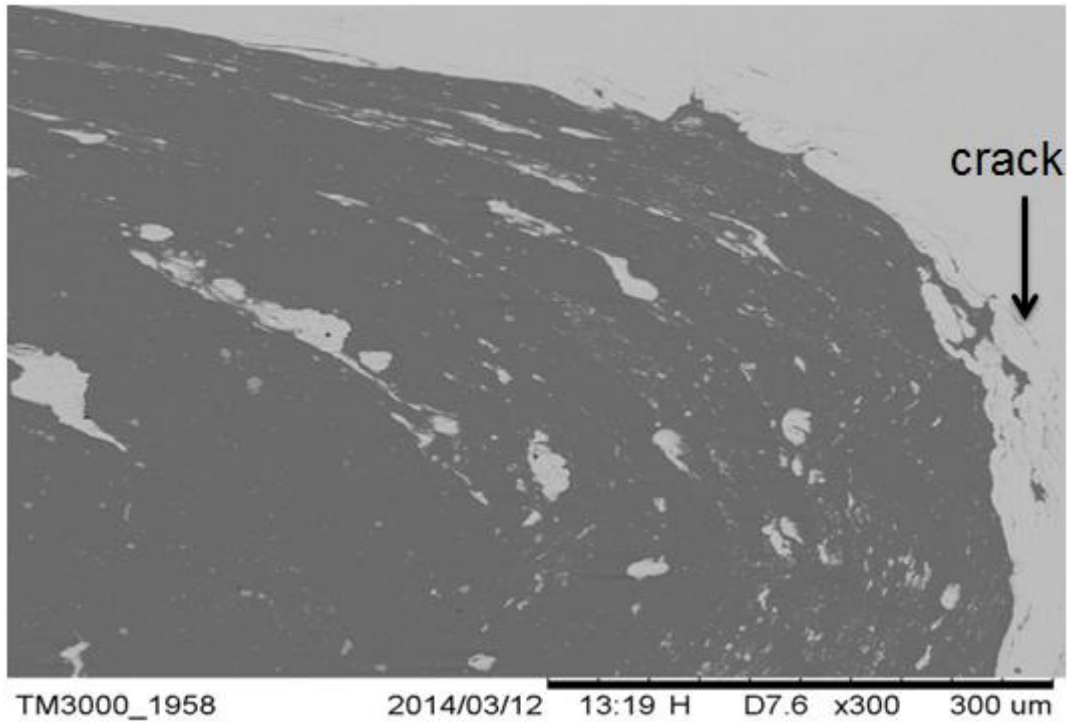


Fig. 7 Interface between AA2024 and Cu10100 (copper is the brighter)

The micro hardness distribution mapped in Figure 8 highlights the influence of the process induced microstructure on the local mechanical properties of the joint. The transition between the AA2024 base material and the Cu10100 base material is clearly visible in correspondence of the weld line. A sharp micro hardness increase was evaluated in the NZ. Despite of the grain refinement, micro hardness values minor than the base material were exhibited, due to the copper particles dispersed within. Some peaks were also measured, attributable to the intermetallic particles observed in the joint.

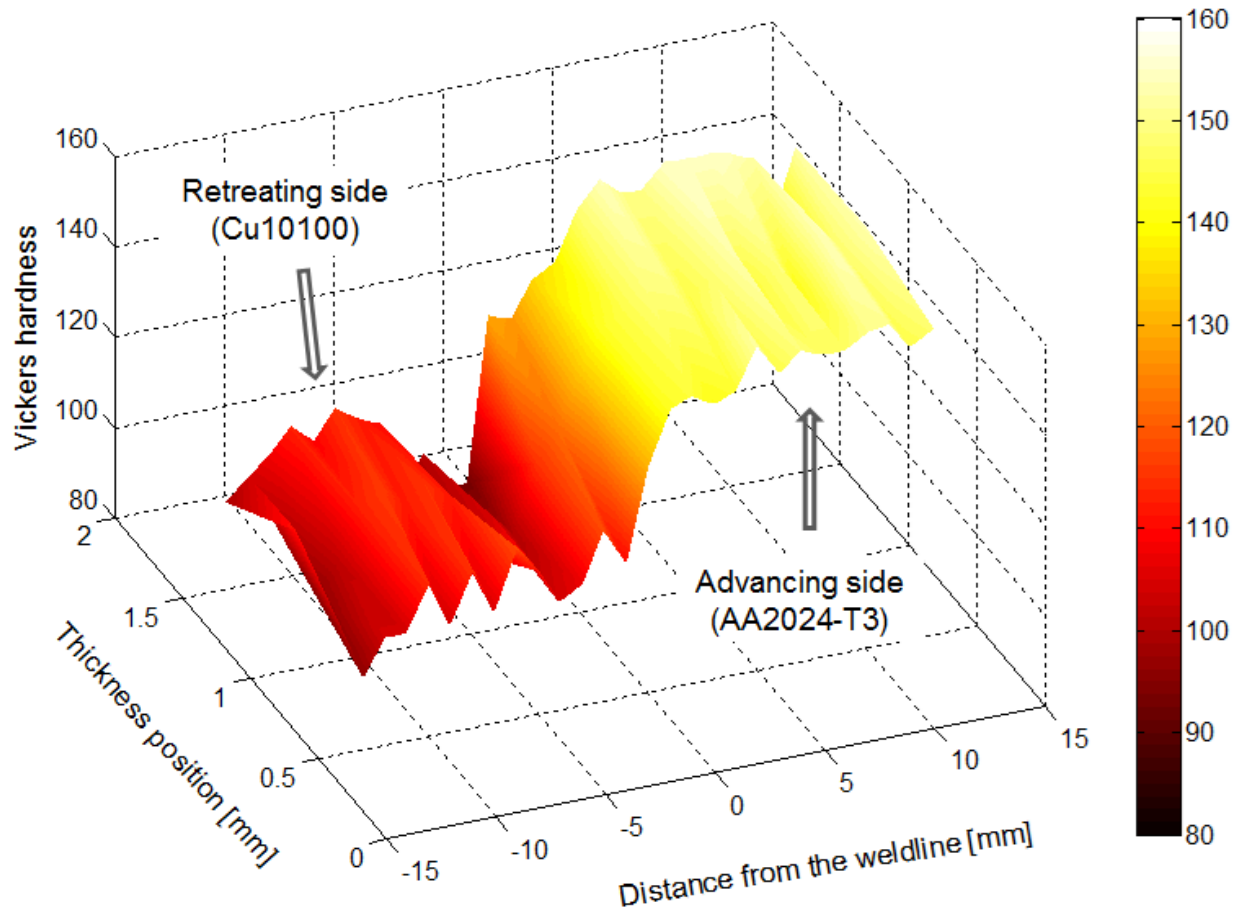


Fig. 8 Microhardness map in the weld bead.

#### 4. Conclusions

On the basis of the experimental campaign carried out the following consideration could be drawn:

- sound AA2024-Cu10100 joints can be obtained by FSW offsetting the pin towards the aluminum side and fixing the copper in the retreating zone;
- the final microstructure exhibits typical FSW features. The NZ consists of a mixture of recrystallized aluminum matrix and deformed/twinned copper particles, resembling an aluminum matrix composite. The distribution of Cu particles with irregular shapes and various sizes appeared inhomogeneous in the NZ, with the formation of a particles-rich zone near the bottom. Onion rings, made of Cu particles dispersed in the Al matrix, were also observed.

1  
2  
3  
4  
5  
6  
7  
8  
9  
10  
11  
12  
13  
14  
15  
16  
17  
18  
19  
20  
21  
22  
23  
24  
25  
26  
27  
28  
29  
30  
31  
32  
33  
34  
35  
36  
37  
38  
39  
40  
41  
42  
43  
44  
45  
46  
47  
48  
49  
50  
51  
52  
53  
54  
55  
56  
57  
58  
59  
60  
61  
62  
63  
64  
65

– Al–Cu IMCs, namely  $\text{Al}_2\text{Cu}$ ,  $\text{AlCu}$ , and  $\text{Al}_3\text{Cu}_4$ , were developed during the welding process, in accordance with the Al–Cu binary equilibrium phase diagram.

– a sharp microhardness increase was measured in the NZ, consistently with the observed microstructure.

## References

1. Ouyang J, Yarrapareddy E, Kovacevic R (2006) Microstructural evolution in the friction stir welded 6061 aluminum alloy (T6-temper condition) to copper. *J Mater Process Technol* 172 :110–122.
2. Murr LE, Flores RD, Flores OV, McClure JC, Liu G, Brown D (1998) Friction stir welding: microstructural characterization. *Mater. Res. Innovation* 1(4):211–223.
3. Murr LE, Ying L, Trillo EA, Flores RD, McClure JC (1998) Microstructure in friction stir welded metals. *J Mater Process Manuf Sci* 7:145–161.
4. Dawes CJ (1977) Micro-friction welding aluminum studs to mild steel plates. *Met Constr* 9(5):196–197.
5. Sun Z, Karppi R (1996) The application of electron beam welding for the joining of dissimilar metals: an overview. *J Mater Process Technol* 59:257 -267
6. Aravind M, Yu P, Yau MY, Dickon HLNg (2004), Formation of  $\text{Al}_2\text{Cu}$  and  $\text{AlCu}$  intermetallics in Al(Cu) alloy matrix composites by reaction sintering. *Mater Sci Eng A* 380:384–393.
7. Liu P, Shi Q, Wang W, Wang X, Zhang Z (2008) Microstructure and XRD analysis of FSW joints for copper T2/aluminium 5A06 dissimilar materials. *Mater Lett* 62:4106–4108.
8. Galvão I, Oliveira JC, Loureiro A, Rodrigues DM (2012) Formation and distribution of brittle structures in friction stir welding of aluminium and copper: Influence of shoulder geometry. *Intermetallics* 22:122-128
9. Abbasi M, Karimi Taheri A, Salehi MT (2001) Growth rate of intermetallic compounds in

Al/Cu bimetal produced by cold roll welding process. *J Alloy Compd* 319:233–241.

10. Squillace A, De Fenzo A, Giorleo G, Bellucci F (2004) A comparison between FSW and TIG welding techniques: modifications of microstructure and pitting corrosion resistance in AA 2024-T3 butt joints. *J Mater Process Technol* 152(1):97–105
11. Mofid MA, Abdollah-Zadeh A, Gür CH (2014) Investigating the formation of intermetallic compounds during friction stir welding of magnesium alloy to aluminum alloy in air and under liquid nitrogen. *Int J Adv Manuf Technol* 71( 5-8):1493-1499.
12. Yilbas BS, Sahin AZ, Kahraman N, Al-Garni AZ (1995) Friction welding of steel–Al and Al–Cu materials, *J Mater Process Technol* 49:431–443.
13. Midling OT, Grong Ø (1994) A process model for friction welding of Al–Mg–Si alloys and Al–SiC metal matrix composites-I. HAZ temperature and strain rate distribution. *Acta Metall Mater* 42(5):1595–1609.
14. Lee WB, SB Jung SB (2003) Void free friction stir weld zone of the dissimilar 6061 aluminum and copper joint by shifting the tool insertion location. *Mater Res Innov* 8(2):93–96.
15. Pratik Agarwal S, Prashanna Nageswaran, Arivazhagan N, Devendranath Ramkumar K (2012) Development of Friction Stir Welded Butt Joints of AA 6063 Aluminium Alloy and Pure Copper. In *Proceedings of the International Conference on Advanced Research in Mechanical Engineering (ICARME-2012)* 13 May 2012, Trivendum, India.
16. Saeid T, Abdollah-zadeh A, Sazgari B (2010) Weldability and mechanical properties of dissimilar aluminum–copper lap joints made by friction stir welding. *J Alloy Compd* 490 652–655.
17. Watanabe T, Takayama H, Yanagisawa A (2006) Joining of aluminum alloy to steel by friction stir welding. *J Mater Process Technol* 178:342–349.
18. Tanaka T, Morishige T, Hirata T (2009) Comprehensive analysis of joint strength for dissimilar friction stir welds of mild steel to aluminum alloys. *Scripta Mater* 61:756–759.
19. DebRoy T, Bhadeshia HKDH (2010) Friction stir welding of dissimilar alloys - a Perspective. *Sci Technol Weld Joining* 15:266–270.

20. Choi DH, Lee CY, Ahn BW, Yeon YM, Park SHC, Sato YS, Kokawa H, Jung SB (2010) Effect of fixed location variation in friction stir welding of steels with different carbon contents. *Sci Technol Weld Joining* 15:299–304.
21. Hussain G, Gao L, Hayat N, Dar NU (2010) The formability of annealed and pre-aged AA-2024 sheets in single-point incremental forming. *Int J Adv Manuf Technol* 46(5-8):543-549.
22. ASM Handbook, Volume 04 - Heat Treating.
23. ASM Specialty Handbook: Aluminum and Aluminum Alloys
24. ASM Specialty Handbook - Copper and Copper Alloys.
25. Carlone P, Palazzo GS (2013) Influence of process parameters on microstructure and mechanical properties in AA2024-T3 friction stir welding. *Metallogr Microstruct Anal.* 2(4):213-222.
26. Carlone P, Palazzo GS (2014) The Influence of Pre-Heating on the Weldability of Pure Copper by FSW. *Open Mech Eng J* 8:177-184.
27. Nandan R, DebRoy T, Bhadeshia HKDH (2008) Recent advances in friction-stir welding – Process, weldment structure and properties. *Prog Mater Sci* 3:980–1023.
28. Reynolds AP (2008) Flow visualization and simulation in FSW. *Scripta Mater* 58:338–342.
29. Xue P, Ni DR, Wang D, Xiao BL, Ma ZY (2011) Effect of friction stir welding parameters on the microstructure and mechanical properties of the dissimilar Al–Cu joints. *Mater Sci Eng A* 528:4683–4689.
30. Tolephih MH, Mahmood HM, Hashem AH, Abdullah ET (2013) Effect of tool offset and tilt angle on weld strength of butt joint friction stir welded specimens of AA2024 aluminum alloy welded to commercial pure copper. *Chem Mater Res* 3(4):49-58
31. Massalski TB (1980) The Al–Cu (Aluminum-Copper) system. *Bulletin of Alloy Phase Diagrams* 1(1):27-33.
32. Chen CY, Chen HL, Hwang WS (2006) Influence of Interfacial Structure Development on the Fracture Mechanism and Bond Strength of Aluminum/Copper Bimetal Plate. *Mater Trans JIM*

47:1232–1239.

1  
2 33. Jiang HG, Dai JY, Tong HY, Ding BZ, Song QH, Hu ZQ (1993) Interfacial reactions on  
3  
4 annealing Cu/Al multilayer thin films. *J Appl Phys* 74:6165–6169.  
5  
6

7 34. Peng XK, Wuhler R, Heness G, Yeung WY (1999) On the interface development and fracture  
8  
9 behaviour of roll bonded copper/aluminium metal laminates. *J Mater Sci* 34:2029–2038.  
10

11 35. Won-Bae L, Yun-Mo Y, Seung-Boo J (2003) The joint properties of dissimilar formed Al  
12  
13 alloys by friction stir welding according to the fixed location of materials. *Scripta Mater* 49:423–  
14  
15 428.  
16  
17

18 36. Xue P, Xiao BL, Ni DR, Ma ZY (2010) Enhanced mechanical properties of friction stir  
19  
20 welded dissimilar Al–Cu joint by intermetallic compounds. *Mater Sci Eng A* 527:5723–5727.  
21  
22  
23  
24  
25  
26  
27  
28  
29  
30  
31  
32  
33  
34  
35  
36  
37  
38  
39  
40  
41  
42  
43  
44  
45  
46  
47  
48  
49  
50  
51  
52  
53  
54  
55  
56  
57  
58  
59  
60  
61  
62  
63  
64  
65

Figure1  
[Click here to download high resolution image](#)

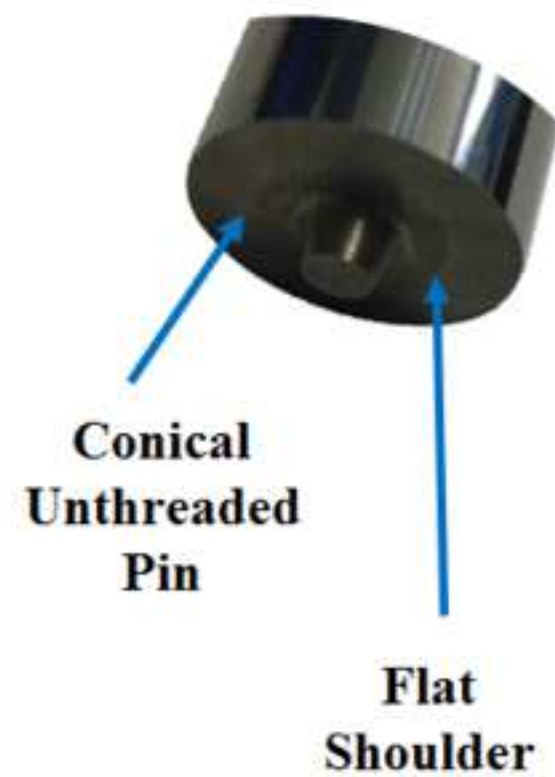
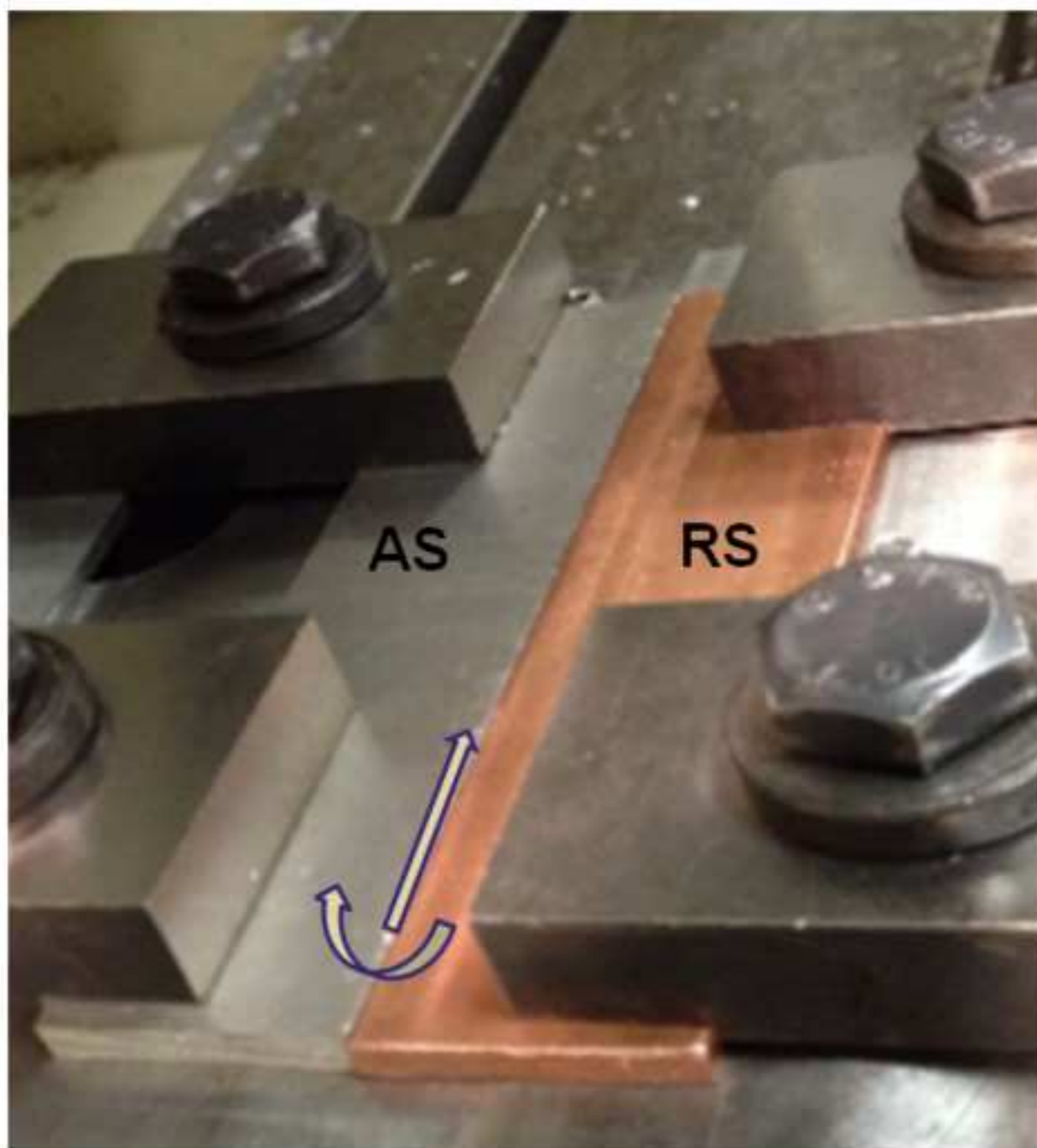
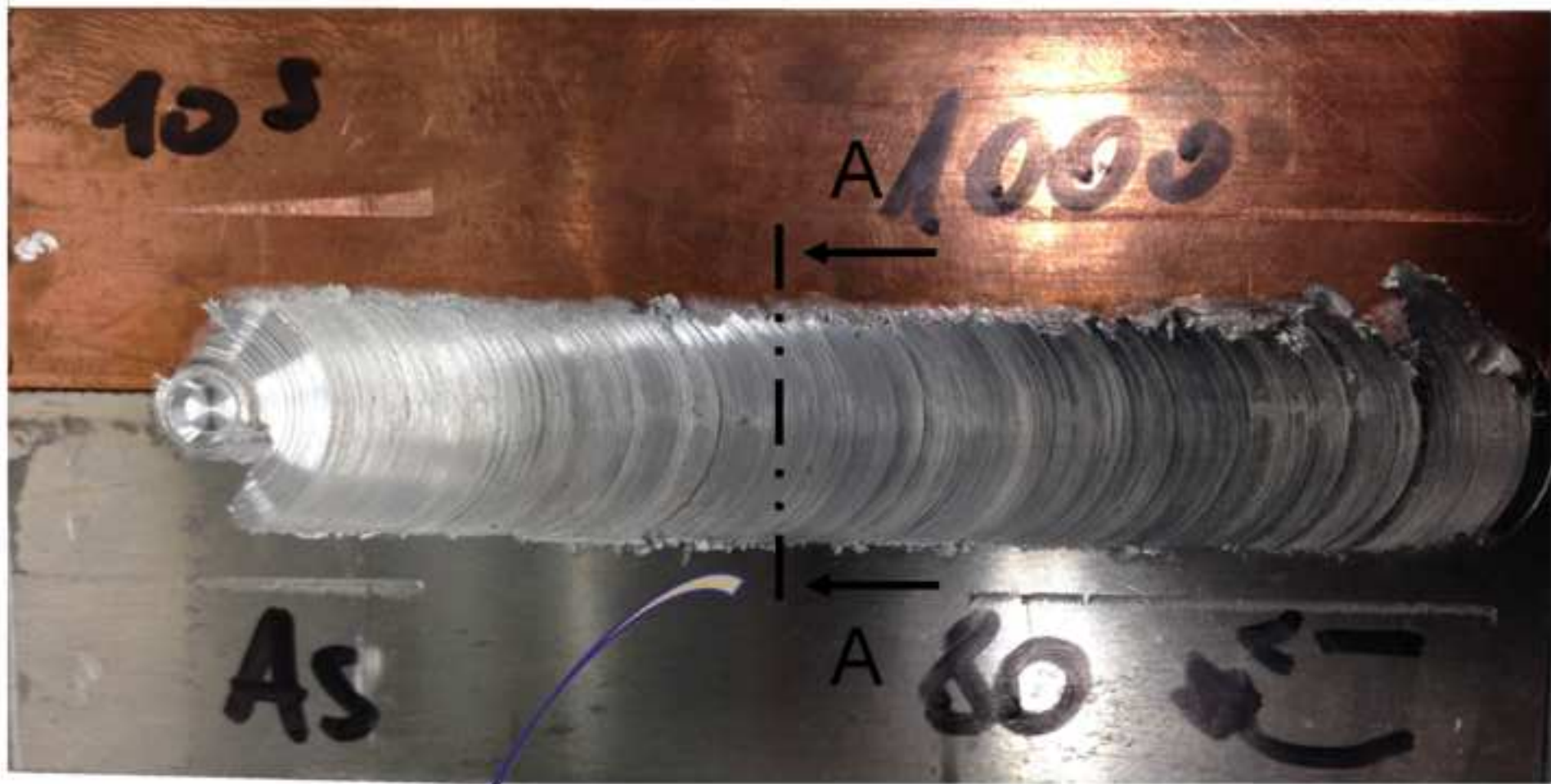


Figure 2

[Click here to download high resolution image](#)



A - A



Figure3  
[Click here to download high resolution image](#)

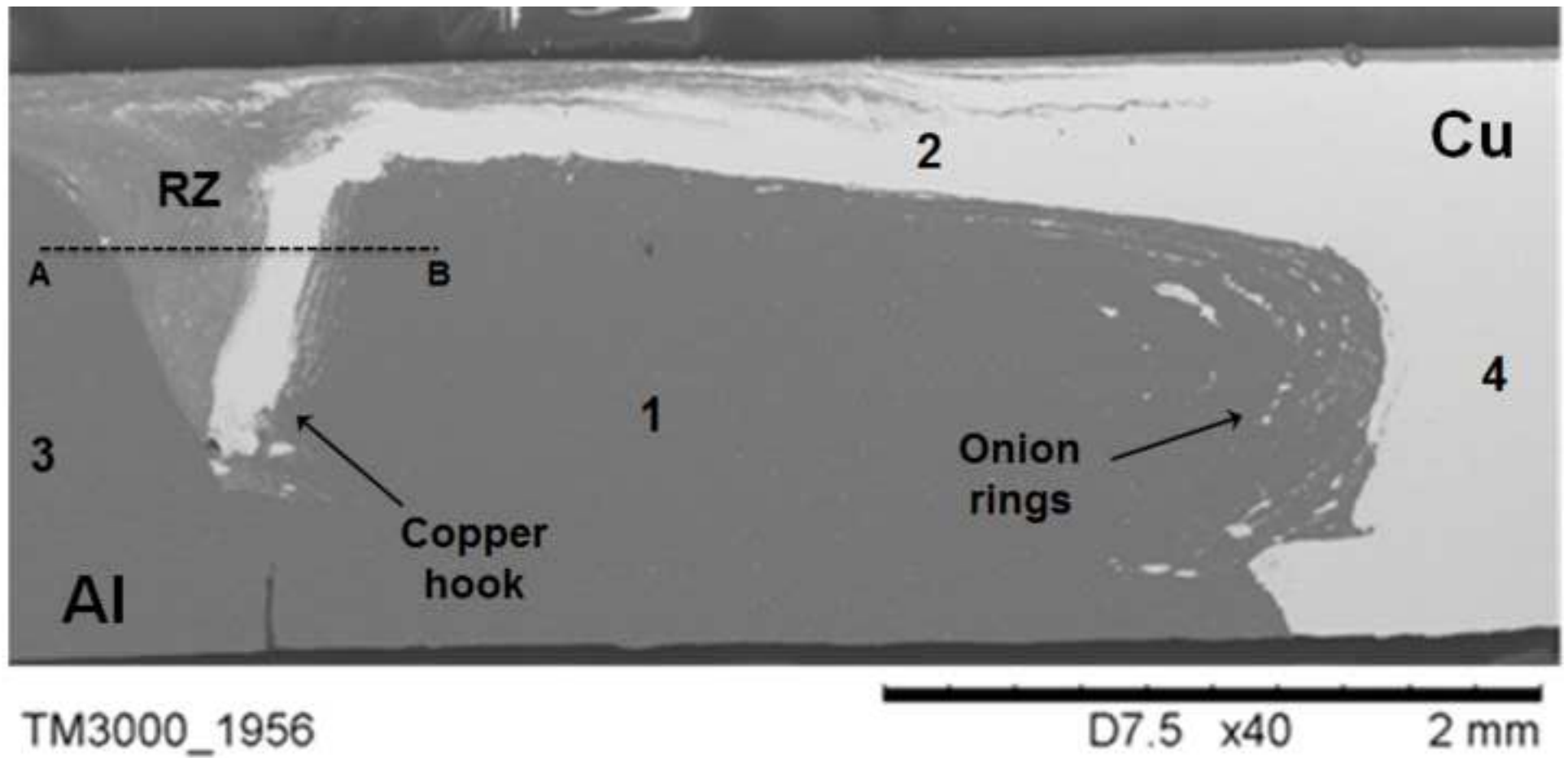


Figure4  
[Click here to download high resolution image](#)

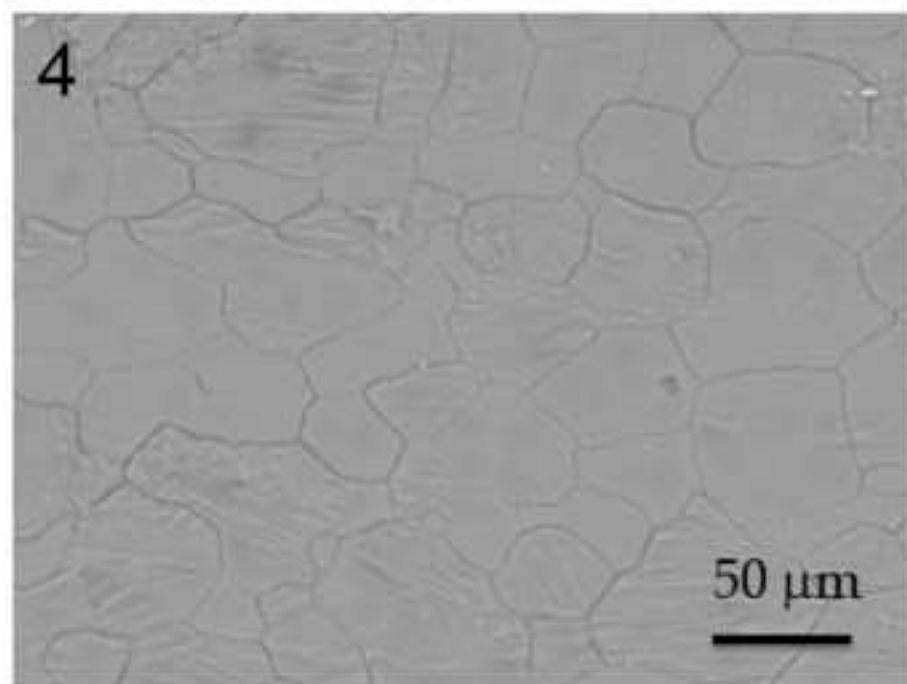
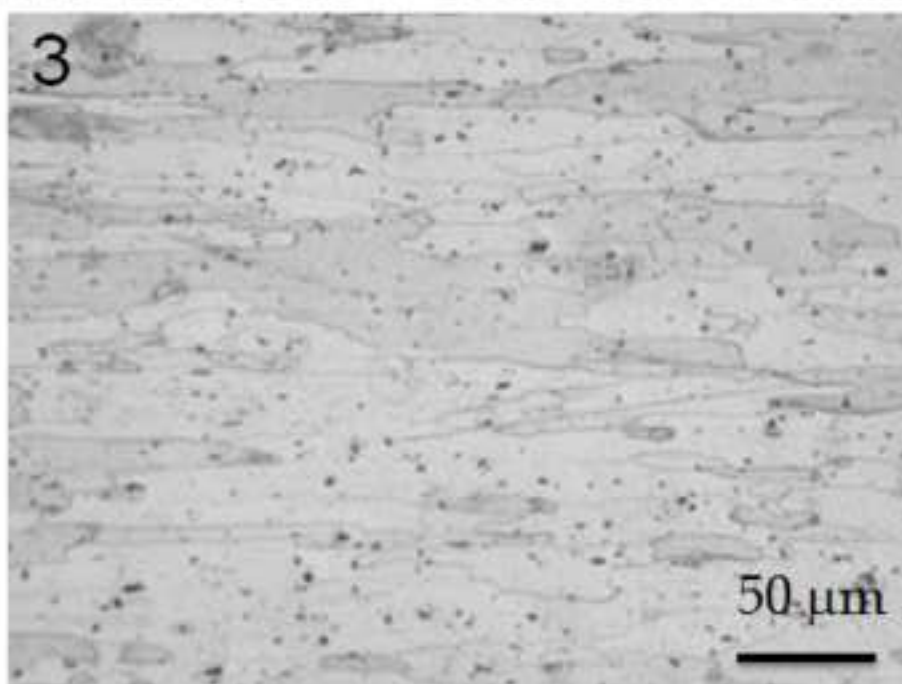
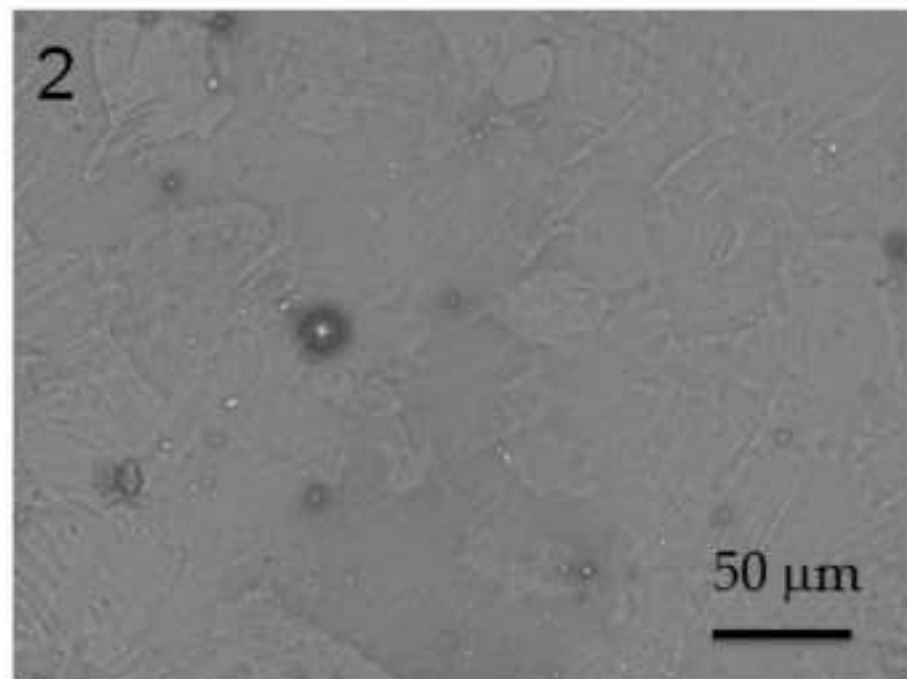
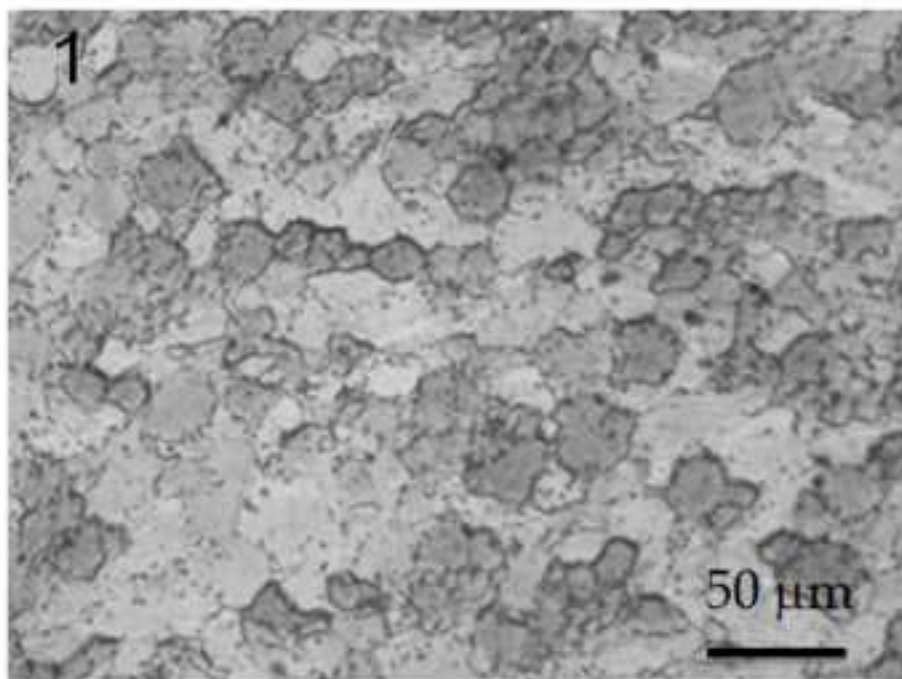
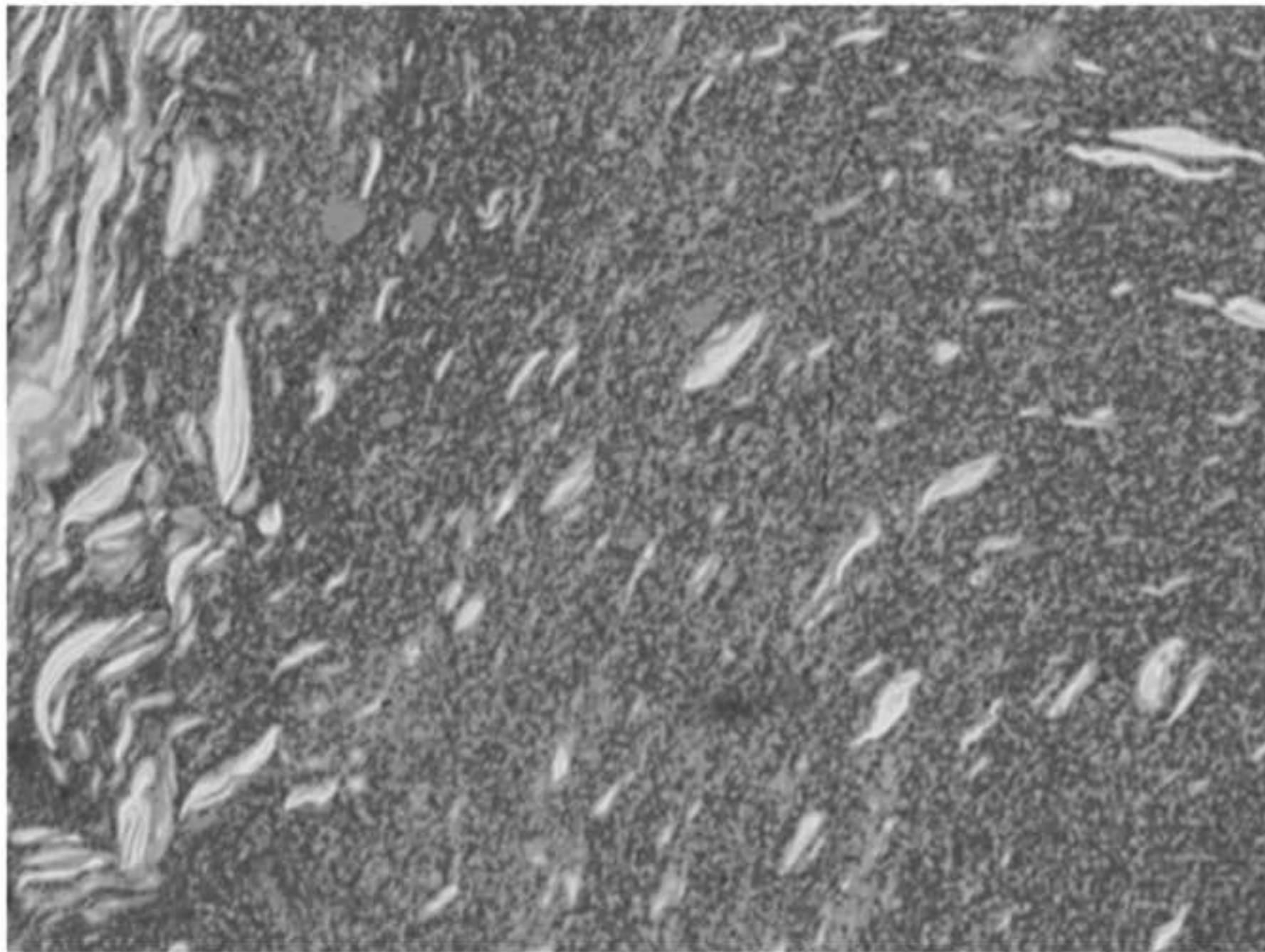


Figure5

[Click here to download high resolution image](#)



TM3000\_1976

2014/03/19

16:15 H

D8.3

x1.5k

50 um

Figure6  
[Click here to download high resolution image](#)

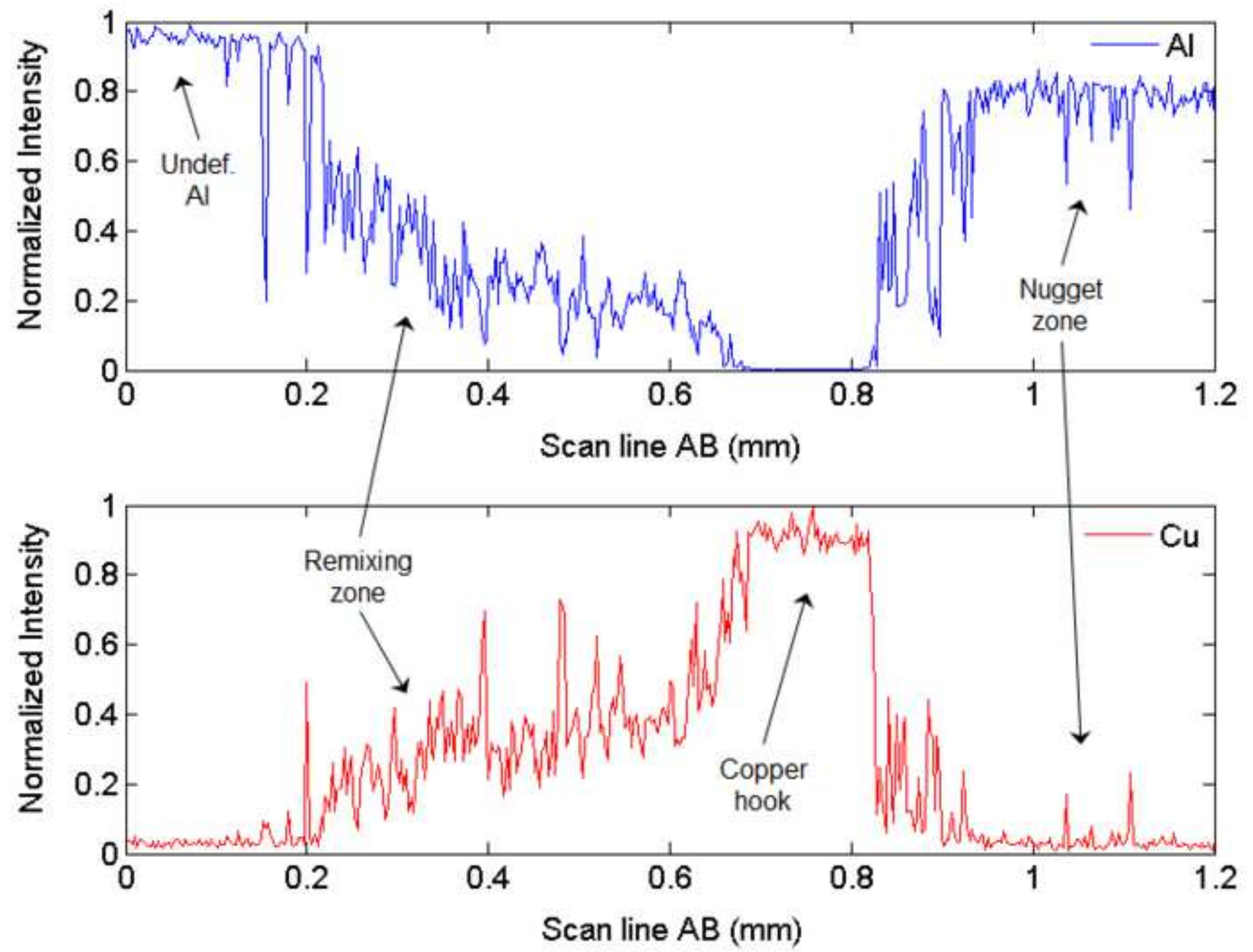
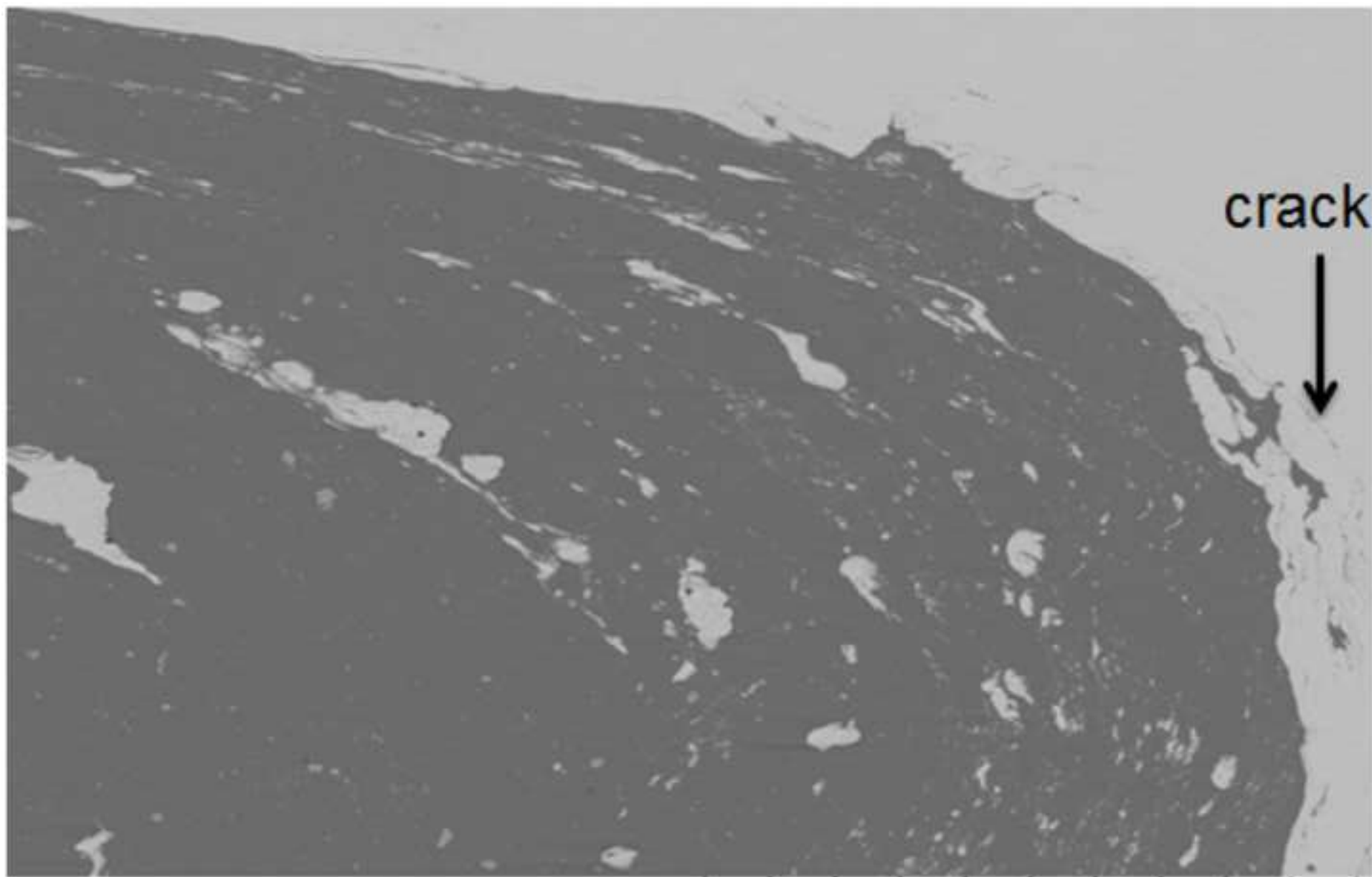


Figure7  
[Click here to download high resolution image](#)



TM3000\_1958

2014/03/12

13:19 H

D7.6

x300

300 um

Figure8  
[Click here to download high resolution image](#)

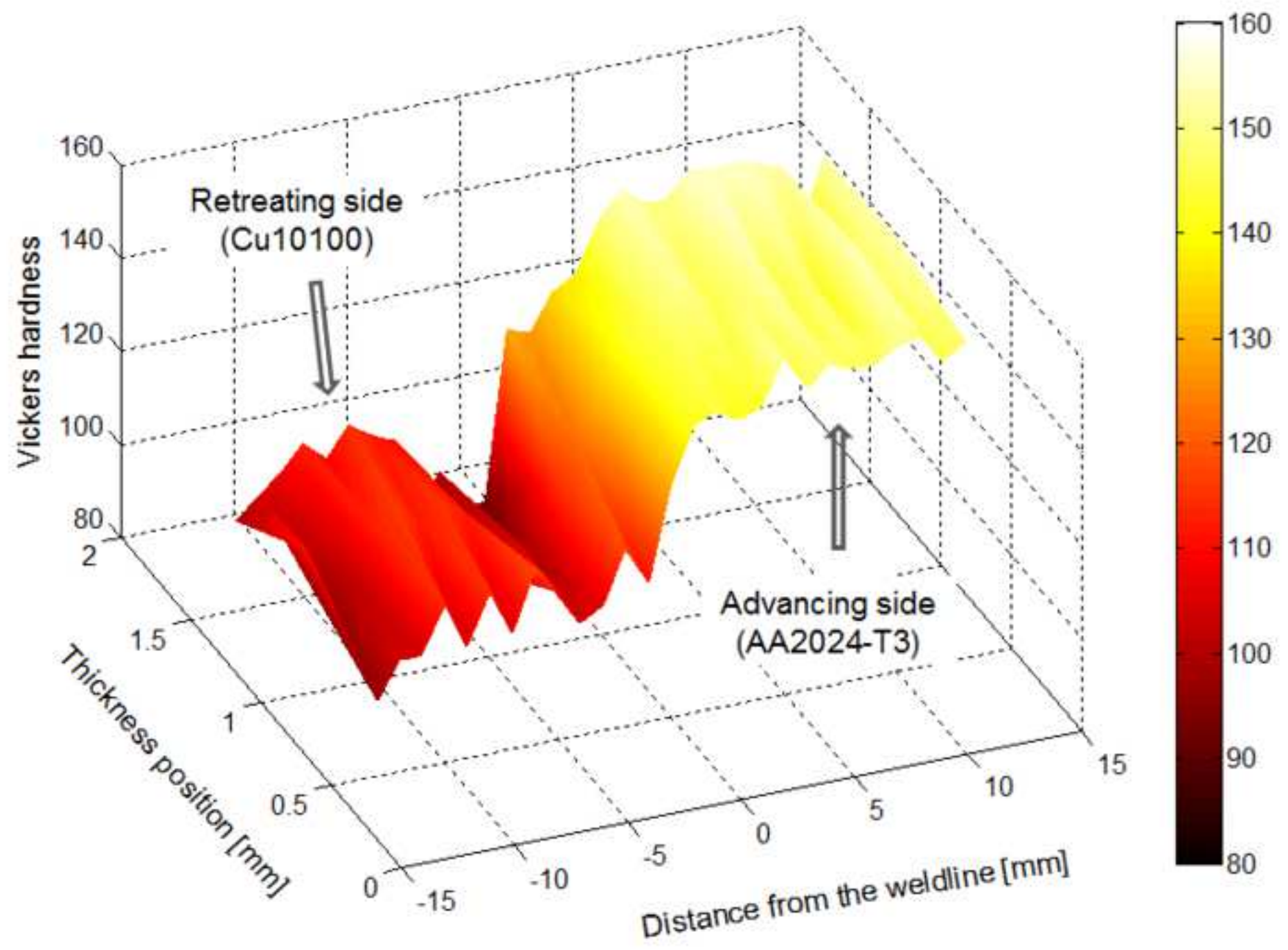


Table 1 – FSW process parameters.

Rotational speed (rpm)	Welding speed (mm/min)	Tilt angle (°)	Tool offset (mm)
1000	80	2	1.3

Table 2 – Chemical composition of IMCs precipitated during FSW process and detected in the NZ

IMC	Al (%)	Cu (%)
AlCu	52	48
Al <sub>2</sub> Cu	65	35
Al <sub>3</sub> Cu <sub>4</sub>	42	58
Al <sub>3</sub> Cu	76	24